Journal of Structural Geology, Vol. 11, No. 6, pp. 689 to 703, 1989
Printed in Great Britain

0191-8141/89 $03.00 + 0.00

Tubular folds and sheath folds: definitions and conceptual models for their development, with examples from the Grapesvare area, northern Sweden

LILIAN SKJERNAA

Institute of General Geology, Øster Voldgade 10, DK-1350 Copenhagen K, Denmark

(*Received* 8 *June* 1988; *accepted in revised form* 28 *February* 1989)

Abstract—Two parameters are used in the classification of highly non-cylindrical folds: the hinge line angle and the ratio of the length of the cone axis to that of the long axis of the cross-section of the structure at the position where the hinge angle was measured.

If in a non-cylindrical fold a cross-section can be selected so that the hinge angle ω measured where the cross-section cuts the cone is less than 90°, and the length of the cone axis x is more than a quarter of the length of the long axis y of the cross-section, the fold is a sheath fold. A tight sheath fold, with $\omega < 20°$ and $x:y > 1$, can be termed a tubular fold. A tubular fold is thus an extreme type of sheath fold.

While sheath folds with $\omega > 20°$ but $< 90°$ and $x:y > 0.25$ but < 1 can be developed by superimposition of layer-parallel simple shear on almost any initial non-cylindrical irregularity, recognizable tubular folds can only be developed from initial non-cylindrical progenitors whose long axes are parallel or almost parallel to the later shearing direction. Such progenitors of tubular folds can be formed by local shortening subperpendicular to the later shearing direction, or they can form in ductile strike-slip zones subparallel to the shearing direction of the later layer-parallel simple shear.

Tubular folds from the Grapesvare area comply to the definition given above, and they occur in a structural setting that is consistent with the models described.

INTRODUCTION

DURING recent years highly non-cylindrical folds have often been described under the names sheath fold and tubular fold. The term sheath fold was introduced by Carreras *et al.* (1977), and has been used by Quinquis *et al.* (1978), Minnigh (1979), Berthé & Brun (1980), Cobbold & Quinquis (1980), Henderson (1981), Mattauer *et al.* (1981), Lisle (1984), Andreasson *et al.* (1985), Faure (1985), Talbot & Jackson (1987), Agar (1988) and Brun & Merle (1988), to mention but a few. Tubular fold is a term that seems to have been used for the first time by Hansen (1971), who provided beautiful illustrations of this type of structure. The term was later adopted by Williams & Zwart (1977), Lister & Price (1978), Andreasson *et al.* (1985) and others. However, some time before any of these papers appeared, Carey (1962, p. 128) described folding "produced by a tongue rising steeply in one place", and he continues: "each surface is shaped like a cap, which rests over a similar cap below it and so down. This is the *paraboloidal* folding". The term paraboloidal was revived by Henderson (1983).

Highly non-cylindrical folds with sharp hinge line bends (hairpin bends—Ghosh & Sengupta 1987) have been amongst structures termed dome and basin structures (Quirke & Lacy 1941, Tobisch 1966), closed folds (Balk 1953), cone and cylinder structures (Ramsay 1958), quaquaversal folds (Quirke & Lacy 1941, Mertie 1957) and eyed folds (Nicholson 1963) or 'eye-folds' (Dalziel & Bailey 1968). In the fold nomenclature of Williams & Chapman (1979) sheath folds are non-cylindrical folds with high R values (see their paper for definition) that pass into isoclinal domes.

DEFINITION OF SHEATH FOLDS AND TUBULAR FOLDS

In spite of all the attention that has been given to sheath folds and tubular folds in recent years, the term sheath fold in particular has been used rather loosely, sometimes to cover almost everything that can give rise to a closed outcrop pattern. Sheath folds were not clearly distinguished from other non-cylindrical folds until Ramsay & Huber (1987) defined a sheath fold as a fold with a hinge line variation of more than 90°, while tubular folds have never been strictly defined at all.

The impression gained by the author from her own field work as well as from the literature (e.g. Dalziel & Bailey 1968, Williams & Zwart 1977, Andreasson *et al.* 1985, Faure 1985) is that in many areas of high deformation, sheath folds with hinge line angles less than 20° are common; many authors mention hinge line angles approaching zero. Furthermore, as will be shown later, such tight sheath folds cannot be produced by the generally accepted mechanisms for the formation of sheath folds in general. Consequently it is considered that a separate term for these folds is warranted, and that the familiar name *tubular fold* is used for such very tight sheath folds. Tubular folds are thus at one end of the spectrum of folds covered by the term sheath fold. Most other sheath folds have much wider hinge angles, and the preconditions for their formation are much less exacting than those for the formation of tubular folds.

Although in the foregoing emphasis has been placed on the hinge angle ω (see Fig. 1a), this angle alone is not enough to define a fold as a tubular fold. Figure 1(b) illustrates this point. In this figure both fold a and fold d have the same value close to 20° for ω, yet while fold a is

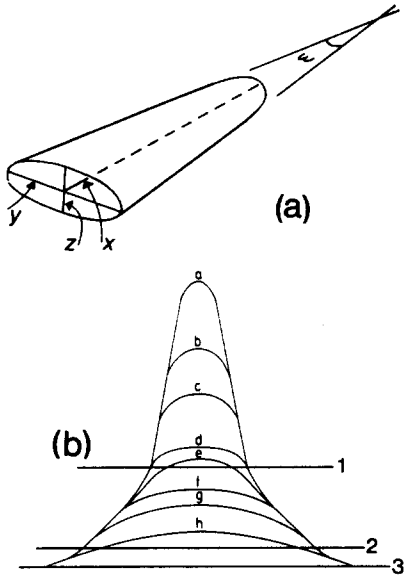

Fig. 1. (a) Geometrical position of the x, y and z axes and the angle ω of a tubular fold. (b) xy sections through non-cylindrical folds. a, b, c and d have $\omega < 20°$ measured at section 1, e, f and g have $\omega < 90°$ measured at section 2 and h has $\omega > 90°$ at section 3. a, b and c have $x:y$ ratios >1, d, e, f have $x:y$ ratios <1 but >1/4. g and h have $x:y$ ratios <1/4. a, b, c are tubular folds, d, e and f are sheath folds, g and h are non-cylindrical folds.

remarkable and is a tubular fold, fold d is neither very remarkable nor is it a tubular fold. In order to classify a fold as tubular, it must be possible to draw a closed cross-section somewhere across the fold so that ω measured at this position is <20° *and* the length of the long axis y of this cross-section is less than the distance of the section from the apex of the fold, i.e. is less than the cone axis x (see Fig. 1a). For sheath folds in general the $x:y$ ratio must be greater than 1:4.

Note that in *describing* as opposed to defining a sheath or tubular fold, the value quoted for ω should be the minimum hinge angle measurable in the fold.

Cross-sections of tubular folds have more or less regular closed forms, and quite often the individual layer boundaries have rather regular elliptical shapes, although they are sometimes attenuated at one end (Figs. 12 and 13). The width to length ratio, i.e. $z:y$ (Fig. 1a), is often between 1:1 and 1:10. This is for example the case in the Grapesvare area, which is described later, and similar ratios seem to be common elsewhere to judge from published descriptions and photos (Hansen 1971, Williams & Zwart 1977, Lister & Price 1978, Minnigh 1979, Cobbold & Quinquis 1980). Williams & Zwart (1977) recorded a range of $z:y$ ratios from 1:1 to 1:25. The longest axis of the cross-section, the y axis, is often close to horizontal or close to vertical, but may have any orientation. Tubular folds (and sheath folds in general) with apices pointing in opposite directions seem to be equally frequent.

Although experience suggests that tubular folds with $z:y$ ratios less than 1:25 are rare, this impression may arise because in practice tubular folds with $z:y$ ratios less than 1:25 are difficult to recognize in cross-sections. However they may be recognized in sections that contain the y axis but make a small angle to the x axis. There seems to be no good reason for putting any restriction on the value of the $z:y$ ratio of a structure to be called a tubular fold.

In conclusion: tubular folds and sheath folds are fold structures with closed cross-sections. Tubular folds have hinge line angle $\omega < 20°$ and $x:y > 1$. For sheath folds the corresponding values are $\omega < 90°$ and $x:y > 1/4$. The definitions of these folds are thus purely geometric.

DEVELOPMENT OF SHEATH FOLDS AND TUBULAR FOLDS

Several models have been proposed to explain the formation of sheath folds. Some of these are discussed below and more than one model may be valid.

In many areas there appears to be a connection between shear zones (e.g. in nappe complexes) and the occurrence of sheath folds (Ramsay & Huber 1987), many of which are tubular folds. It is therefore reasonable to relate these phenomena and suggest that the mechanism of formation of sheath folds and tubular folds has something to do with simple shear deformation, at least in these environments.

It should however be emphasized that under certain circumstances sheath folds may form in other deformational regimes, such as those of pure shear, either plane strain or constrictional (Borradaile 1972), diapirism or three-dimensional differential (i.e. non-planar) flow (cf. Bhattacharji 1958, Nicholson 1963, Hansen 1971, Ramsay & Sturt 1973). For reasons of space these cases are not considered here.

The models discussed below all relate to deformational regimes with a dominant component of subhorizontal simple shear as found in some nappe complexes. The results are of course equally valid for shear zones with other orientations. An explanation of the formation of sheath folds that has gained broad acceptance during the last few years, almost to the point where it is used unquestioningly as *the* explanation (e.g. Leon & Choukroune 1980, Henderson 1981, Mattauer *et al.* 1981, Malavieille 1987), was given by Cobbold & Quinquis (1980) as their model 1. Cobbold & Quinquis showed that sheath folds develop when layers containing small irregularities, such as gentle bumps and dents, are involved in an overall layer-parallel simple shear.

A similar model was proposed by Quinquis *et al.* (1978), Minnigh (1979) and Hibbard & Karig (1987) (see also Ramsay 1980 and Ragan 1985, p. 255). These authors have suggested that the "initial irregularities" were syn-shear derived, slightly non-cylindrical folds which had main axial direction at right angles to the shearing direction of an overall layer-parallel mainly simple shear deformation.

Both these models may afford satisfactory explanations for the occurrence of non-cylindrical folds and sheath folds in shear zones. Tubular folds that fulfil the requirements of the definition given in the foregoing cannot, however, have formed by either of the processes

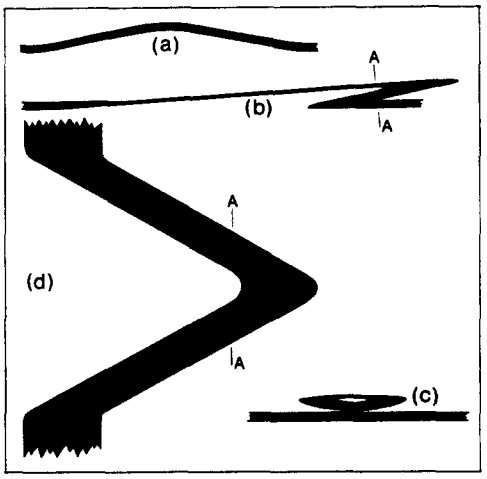

Fig. 2. (a) Section through a circular bump (or low dome) before shearing; (b)–(d) are sections along the xz plane, the yz plane and the xy plane, respectively, of the sheath fold that has developed from the circular bump after a 'layer-parallel' dextral shear of $\gamma = 10$. A–A in (b) and (d) show the position of (c).

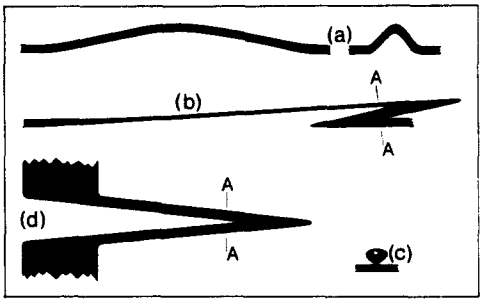

Fig. 3. (a) Longitudinal and cross-sections through an oval bump (or an open periclinal fold) before shearing; (b)–(d) are sections along the xz plane, the yz plane and the xy plane, respectively, of the tubular fold that has developed from the oval bump after a 'hinge parallel' dextral shear of $\gamma = 10$. A–A in (b) and (d) show the position of (c).

described, except for tubular folds with extremely low $z:y$ ratios that would hardly be recognizable in outcrops. The theoretical background for this conclusion is treated in detail below.

In the following, folds with flat-lying axes either subperpendicular or subparallel to the later simple shear deformation are termed longitudinal and transverse respectively. Note that longitudinal and transverse refer to the length of the nappe complex, or to the orogen.

Transverse structures, such as oval bumps and dents or anticlines and synclines with culminations and depressions respectively and with their main axes parallel to, or at a small angle to, the shearing direction, can develop into tubular folds with $z:y$ ratios comparable to those commonly seen in nature, if they are exposed to sufficient overall layer-parallel simple shear.

Figure 2(a) shows a cross-section through a gentle dome with circular ground plan and interlimb angle 160°. When this dome has been horizontally sheared with $\gamma = 10$ (dextral shears are given positive values) it will develop into a sheath fold. Figure 2(b) shows a section through this fold parallel to the ac-kinematic plane which is the xz plane of the fold (compare with Fig. 1). Figures 2(c) & (d) are sections parallel to the yz and the xy planes of the fold, respectively. The ω angle is 58.9° (seen in Fig. 2d) while the lowest interlimb angle as seen in Fig. 2(b) is 9.4°. The $z:y$ ratio can be seen from Fig. 2(c) and is 0.145 (1/7). The fold is a sheath fold according to the definition used in this paper. To make a tubular fold from the original dome in Fig. 2(a), a shear of $\gamma = 32$ would be needed. The angle ω would then be 20°, the smallest interlimb angle ~0.6° and the $z:y$ ratio ~1:31. The tubular fold would be extremely thin and would hardly be identifiable.

Figure 3(a) shows sections parallel to, and at right angles to, the main axis of a transverse anticline with an axis culmination, i.e. a periclinal fold. The hinge line angle (measured in the left section) is 160° and the interlimb angle is 90°. Figures 3(b)–(d) show the sections parallel to the xz, the yz and the xy planes, respectively, after a shear of $\gamma = 10$ parallel with the axis. The angle ω (in Fig. 3d) is 11.36° and the smallest interlimb angle (in Fig. 3b) is 9.4° while the $z:y$ ratio is 0.82 (5:6). The structure is thus a tubular fold.

From the equations derived in the Appendix, a diagram (Fig. 4) has been constructed for the case of a layer-parallel simple shear superposed on initially upright circular domes (or basins). α_0 and α are the initial and final interlimb angles measured in the xz plane (which is parallel to the ac-kinematic plane) while β_0 and β are the interlimb angles in the xy plane (see Figs. A1 and A2 in the Appendix). In this case β is always the largest interlimb angle and is thus the hinge line angle in the final fold, i.e. $\beta = \omega$.

It can be inferred from Fig. 4 that for gentle domes which have large α_0 and β_0 values, tubular folds can only form when γ is large, in which case the $z:y$ ratios are small. Most natural tubular folds have α, β and $z:y$ values comparable to those in the lower left quarter of the diagram, and if they evolved from initial circular deflections, these must have been rather steep sided. A well developed dome and basin pattern may evolve to a system of tubular folds, but minor layer irregularities cannot. The open triangle in Fig. 4 refers to the case shown in Fig. 2.

In the case of upright periclinal folds with the main axes of the folds either parallel to the shearing direction ($\alpha_0 > \beta_0$) or at right angles to it ($\alpha_0 < \beta_0$) (i.e. transverse and longitudinal folds, respectively) the same graph may be used. While both α and $z:y$ in this case are functions of α_0 and of the intensity of the shear, the $z:y$ ratio is also dependent on the initial length:width ratio of the oval ground plan of the original periclinal fold (see equations A11, A12, A1 and A2 of the Appendix). l_1 is measured parallel to the shearing direction and l_3 perpendicular to it. Transverse periclinal folds thus have $l_1:l_3$ greater than unity. The β angle is a function of β_0 and the shear value (see equation A6 in the Appendix).

To use Fig. 4 in the case of a periclinal fold the value of α and of $z:y$ should be read off using the appropriate values of α_0 and γ. The true value of $z:y$ is found by multiplying the read-off $z:y$ value by $l_1:l_3$. The value of β is found in the same diagram from appropriate values

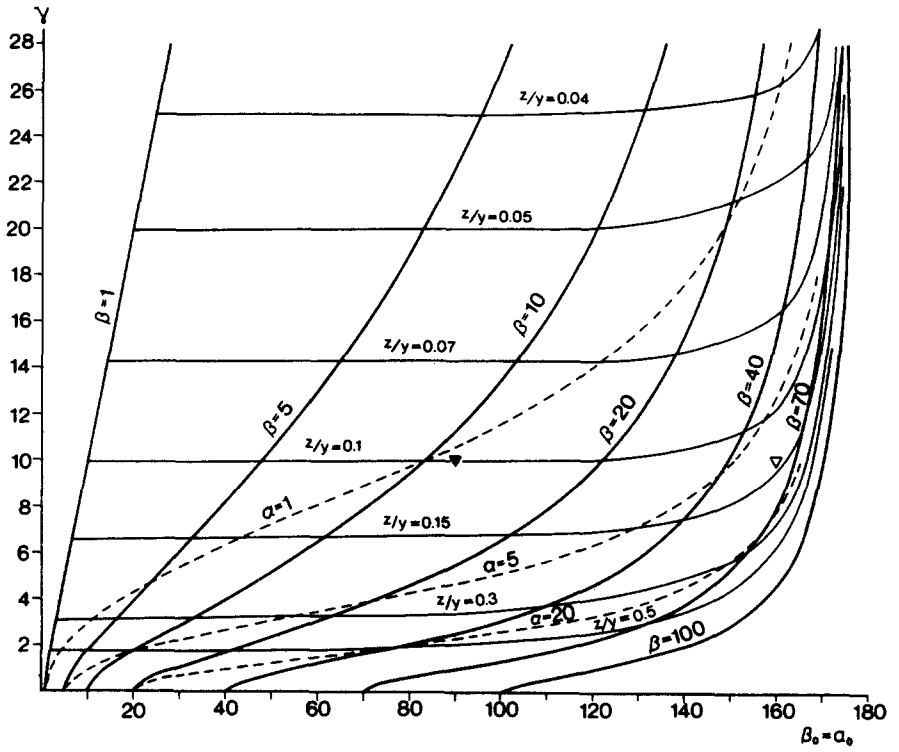

Fig. 4. Diagram showing values of α, β and $z:y$ as functions of $\alpha_0 = \beta_0$ (see text and Figs. A1 and A2 in the Appendix) and γ for the case of initial circular domes or basins overprinted by an overall layer-parallel simple shear, in this case $\beta = \omega$. The diagram may also, with some modifications discussed in the text, be used for initial periclinal folds that are sheared parallel with or orthogonal to their axes. The triangles refer to Figs. 2 and 3; see text for explanation.

of β_0 and γ. ω is equal to either α or β (whichever is largest). The open triangle in Fig. 4 gives α and the filled triangle β for the case illustrated in Fig. 3. To find the $z:y$ value in this case, the value read off at the open triangle should be multiplied by $l_1:l_3$ which in this case is 5.65.

It is seen that from initial periclinal transverse folds tubular folds comparable to those found in nature are easily developed, while this is not possible from an initial longitudinal fold which has $l_1:l_3$ less than unity.

Associations of tubular folds and transverse folds

As shown above, minor initial deflections in otherwise plane layers that have been subjected to layer-parallel simple shear may be the source of non-cylindrical folds, sheath folds and, in special cases (if the deflections are more or less parallel to the shearing direction), tubular folds. Such folds might be expected here and there in an otherwise planar sequence. There should be no cylindrical folds associated with them.

It is however a characteristic feature of many areas that tubular folds are intimately associated with a subparallel system of cylindrical or slightly curved folds (e.g. Mattauer *et al.* 1981, Ewans & White 1984, Gaudemer & Tapponier 1987, Malavieille 1987), see also Figs. 12 and 13. Such patterns may result from a simple shear superimposed on transverse folds with enveloping surfaces (overall layer orientation) parallel or subparallel to the shear plane. Occasional axial culminations and depressions, or interference structures with longitudinal folds, may give rise to tubular folds (Figs. 5, 6 and 8).

Transverse fold systems consisting of major and minor recumbent folds have been described from many places (e.g. Carmignani *et al.* 1978, see Olesen & Sørensen 1972 for other references). Such folds are frequent in the Grapesvare area, which is described in a later section, as well as in the rest of the Seve nappe complex and in fact in most of the Scandinavian Caledonides (see articles in Gee & Sturt 1985).

It is hardly realistic, as many have done (Bryant & Reed 1969, Williams 1978, Ewans & White 1984 among many others), to consider these folds as having been passively rotated from an initial longitudinal orientation during an overall layer-parallel simple shear deformation (Figs. 8a & b) (see also Ghosh & Sengupta 1984, Hibbard & Karig 1987). Such a reorientation would imply simple shear values not less than γ = 100–150. The resulting extensions along the fold axes would probably exceed 1000% (Skjernaa 1980) and the extension in the fold limbs would be much larger. The exact figures are very dependent on the original and final orientations of the folds, but certainly strain values of this magnitude would cause the folds to be obliterated, or at least only remnants of them would have been preserved, probably as attenuated lenses of rootless, intrafolial folds (cf. Meneilly & Storey 1986). Obliteration of folds also occurs in glaciers, e.g. in the salt glacier at Kuh-e-Namak in Iran (Talbot 1979, Talbot & Jackson 1987) when folds with axes initially oriented across the glacier are reoriented towards the flow direction.

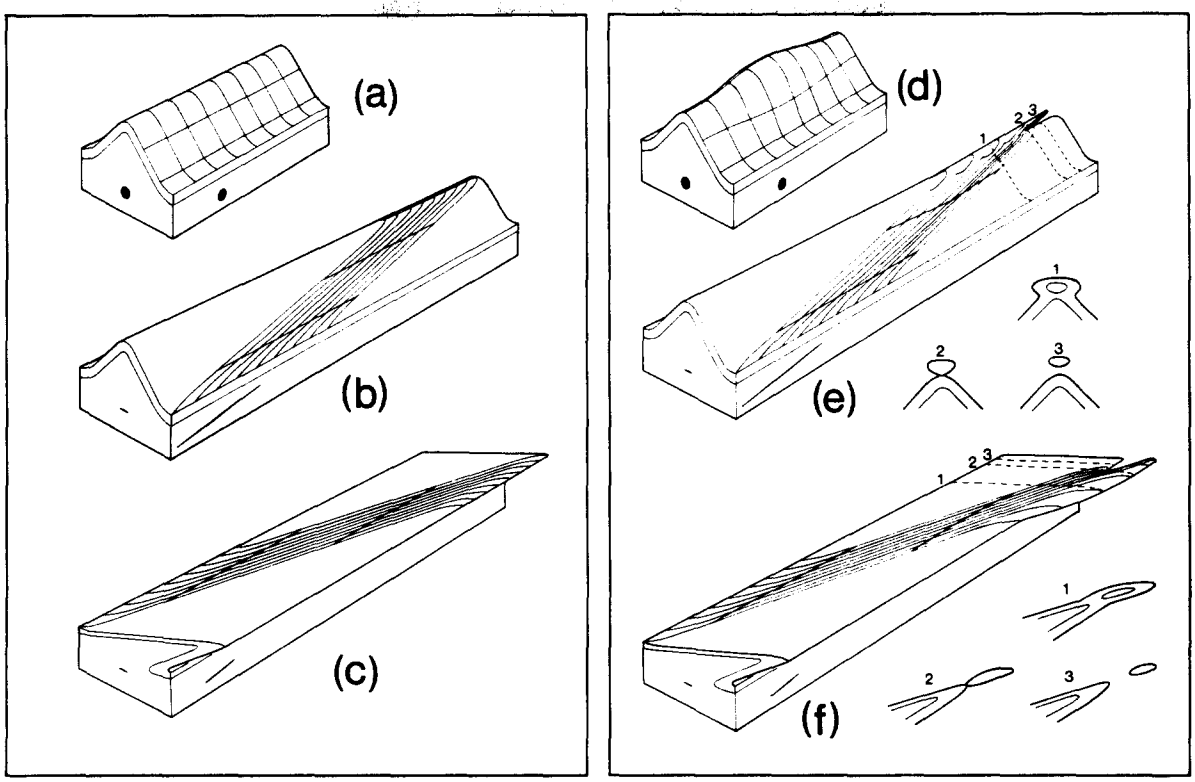

Fig. 5. (a) Cylindrical fold before shearing, (b) after a horizontal hinge line-parallel dextral shear and (c) after a horizontal shear at 15° to the axial direction (γ = 10). The lines on the upper surface are the deformed grids shown in (a). The ellipses at the fronts and sides of the blocks are strain ellipses in these sections. (d)–(f) are similar to (a)–(c) except that the initial fold in (d) is periclinal. Tubular folds are developed in (e) and (f); 1, 2 and 3 are sections. Note that all the blocks are drawn in perspective.

Brun & Merle (1988) gave an example of longitudinal folds which retained their orientation and even their cylindricity after large simple shears.

Other mechanisms, probably implying axial parallel shortening, must therefore be sought to explain indisputable rotations of folds through almost 90° in a plane that is parallel to the overall layer orientation.

In cases where the initial fold axes are parallel to the later shearing direction, cylindrical folds will maintain both their axis orientation and their appearance in cross-section, and are thus capable of surviving very intense shearing; this is shown in Figs. 5(a) & (b). A stretching lineation will develop on the limbs of the folds, and for large shears it will rotate to subparallel the fold axis (for γ = 20 the angle between the stretching lineation and the fold axis becomes less than 3°).

If the axes of the cylindrical folds formed a small angle to the later shearing direction, but still lay in the shear plane, they become overturned and tightened and the limbs become thinned (see Fig. 5c). The orientation of the axes is maintained and the stretching lineation in the limbs of the folds becomes subparallel to the fold axes for large shears.

If the initial transverse folds were not cylindrical but for example contained anticlinal axial culminations (Fig. 5d), these would evolve to form sheath folds and eventually tubular folds during the simple shear deformation. This case is illustrated in Figs. 5(e) & (f) for axis-parallel shear and shear at a small angle to the fold axis, respectively. In the first case the cone axis of the tubular fold becomes subparallel to the fold axis of the cylindrical parts of the fold when large shears are superimposed (for α_0 = 160° and γ = 20 the angle between the cylindrical fold axis and the tubular fold cone axis becomes about 3°). In the second case (Fig. 5f) the cone axis becomes subparallel to the shearing direction. The small angle between the cone axis of the tubular fold and the axis of the cylindrical parts of the fold approximates the initial angle between fold axis and shearing direction. However, if the fold axis did not start in the shear plane, but had a low plunge to the rear in relation to the shearing direction it would slowly rotate towards this direction and eventually approach the cone axis of the tubular fold. The same result may be achieved if the orientation of the shear plane was not completely constant during the shearing event. Figure 6 shows examples of various cross-sectional patterns that may develop from different initial fold geometries when slightly oblique simple shears are superimposed on them.

It would be possible to set up mathematical relations for cases of oblique simple shear, but the equations would be long and tedious. A lucid way of representing the result of simple shear deformation superposed on periclinal folds with their main axes at an angle θ to the shearing direction is to draw a structural contour map for the pre-shear structure. Each structure is then translated along the shearing direction by a distance that is found by multiplying the γ value by the distance to a reference shear plane (see Fig. 7). From the resulting structural

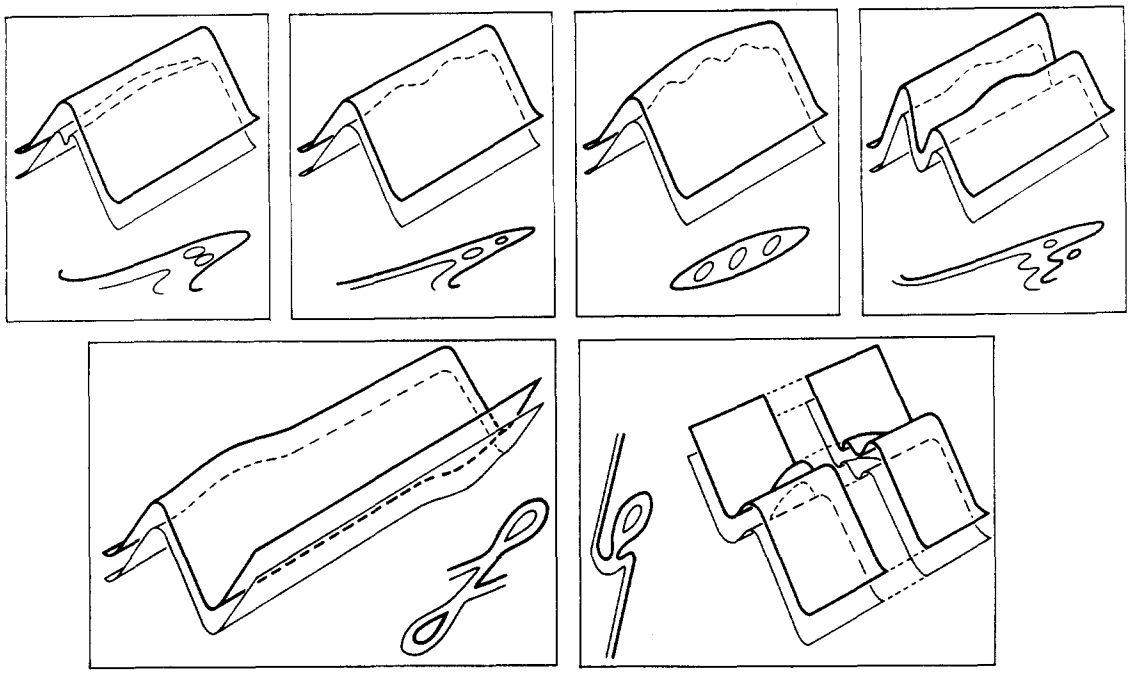

Fig. 6. Examples of different initial geometries which may give rise to tubular folds when horizontal shears parallel to, or at a small angle to, the main axial directions are superimposed on the structures. Possible cross-section patterns after slightly oblique shears are shown.

contour map for the final structure, sections may be constructed to measure ω, $z:y$, etc. For a specific initial geometry of a periclinal fold and a fixed value of γ, increasing values of the angle θ between the fold axis and the shearing direction will result in an increase of ω and a decrease of $z:y$ (Figs. 7b & c). Tubular folds with $z:y$ in the order of 1 : 1–1 : 25 only form when the θ values are small. Non-cylindrical fold segments with a steep hinge line plunge in one direction (Fig. 7d), produce tubular folds with smaller values of ω for similar values of γ and θ if simple shear is oblique (see Figs. 7c & f). Transverse periclinal folds similar to that in Fig. 7(e) may be formed above circular obstacles on the floor of the shearing system and evolve into sheath folds and tubular folds (Brun & Merle 1988). A similar pattern may arise when asymmetric longitudinal folds override the crests of larger transverse folds, or vice versa (Figs. 8c & f) (see also Platt & Lister 1985).

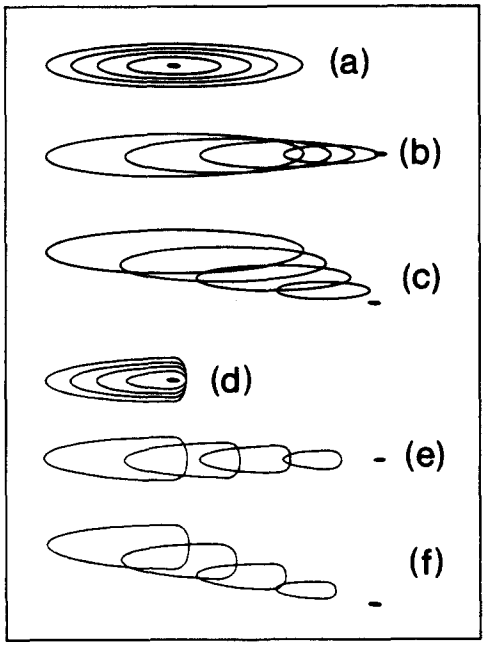

Fig. 7. Structural contour maps showing (a) unsheared periclinal antiform with equal hinge line plunges in both directions. (b) The same anticline after horizontal shearing (γ = 10) parallel to the main axial direction. The tubular fold developed has $\omega = \beta = 11°$. (c) The periclinal fold from (a) after a horizontal shear (γ = 10) in a direction making an angle θ = 15° to the main axis. The sheath fold that has developed has ω = 22°. (d) Unsheared periclinal antiform with vertical hinge line at one end. (e) The anticline from (d) after a shear (γ = 10) in the direction of the main axis; ω = 11° in the resulting tubular fold. (f) The anticline from (d) after an oblique shear (θ = 15°); a tubular fold with ω = 11° has developed.

Figures 8(a) & (c)–(g) show initially subhorizontal longitudinal folds that are first rotated to a moderately or steeply dipping position by the overprinting of transverse folds. During the subsequent simple shear they are rotated relatively rapidly (Skjernaa 1980) towards the shearing direction. They end up as transverse folds themselves and at the same time produce tubular folds at their culminations above the crest of the major transverse fold. The theoretical cross-sections closely resemble some natural outcrop patterns (cf. Figs. 8k & j).

Origin of progenitors of tubular folds

Tubular folds are mostly found in rock sequences built up of layers with alternating rheological properties. Such layered sequences seem to buckle when they are shortened while they behave much more passively, i.e. by homogeneous thinning, when extended. In many areas, e.g. the Grapesvare area, boudinage and necking are seldom seen, except when exceptionally competent layers are incorporated.

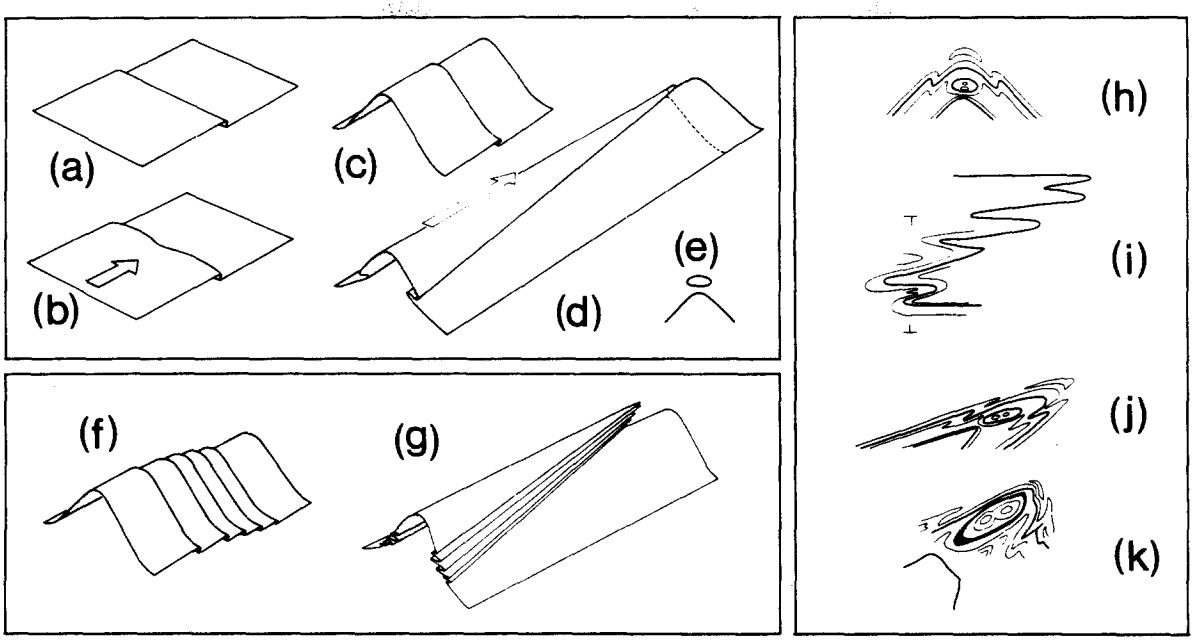

Fig. 8. (a) and (b) A layer containing a fold is exposed to a layer-parallel shear at right angles to the fold axis. The fold axis may become slightly non-linear, but no real rotation takes place. (c) The layer in (a) becomes folded around a fold axis at right angles to the first fold. (d) Shearing along the new fold axis rotates the first fold, and a tubular fold is formed at the cusp bend of the first fold axis. (e) Section along the dashed line in (d). (f) and (g) Similar to (c) and (d), but several early folds are involved. (h) and (i) Sections perpendicular and parallel to the main axis in (g). Marks in (i) show position of (h). (j) Similar to (h) except that in this case the shearing has been slightly oblique. (k) Sketch of the structures from the Grapesvare area shown in Fig. 12 (d); compare with (j).

The initial structures that are the progenitors of tubular and other sheath folds probably often originated from the overprinting of structural elements. The fold phases that produced these structures may predate the shearing process and nappe emplacement, but the folds may equally well have developed at different times during nappe emplacement as a consequence of local heterogeneities in the shearing process. The previous existence of some kind of transverse fold seems to be a prerequisite for the formation of a tubular fold in an overall layer-parallel simple shear regime.

It cannot be too strongly emphasized that 'fold phases' are not isochron time markers, especially not when they are formed by a rotational deformation (Williams & Zwart 1977, Coward & Potts 1983, Coward 1984).

Where and when each type of structure forms are dependent not only on the rheological properties of the layers and the homogeneity of the flow (Marcoux *et al.* 1987), but also on the local orientation of the deforming surfaces in relation to the shear plane and the shearing direction (Escher & Waterson 1974, Ramberg & Ghosh 1977, Skjernaa 1980) and on local deviations from plane strain, i.e. whether or not there is a longitudinal strain along one or more of the kinematic axes. The diachronism of fold generation is well illustrated in flowing and deforming systems such as glaciers (Hudleston 1977, Talbot 1979).

Price (1972) gave an account of "diachronism in tectonic overprinting" and on the basis of the Prandtl cell model he examined the internal flow both in glaciers and in orogenic nappes. This model involves a shift from extension to compression along the kinematic *a*-axis when a volume of rock moves from the internal towards the external parts of the deforming system. The latter situation gives rise to a system of longitudinal folds, while transverse folds are not developed (cf. the experiments described by Brun & Merle 1988).

The Prandtl cell model is a two-dimensional plane strain model that does not consider longitudinal strain along the kinematic *b*-axis. However, longitudinal strain along the nappe length is possible, as for example in response to culminations and depressions in the floor of the nappe (Butler 1982, see also Sanderson 1982). A longitudinal shortening may lead to the formation of transverse folds.

Heterogeneities within the deforming complex, for example competent boudins, or at its boundaries may cause the stream lines of the flow to crosscut the layering, and folds with axes at a large angle to the flow direction are then formed (Hudleston 1977, Cobbold & Quinquis 1980, Ghosh & Sengupta 1984, Hanmer 1986, Talbot & Jackson 1987, Brun & Merle 1988). These folds may overprint or be overprinted by transverse folds (Fig. 8) and result in superimposed structures which are likely progenitors of folds or, provided they have the right geometrical properties as described in the foregoing, of tubular folds.

Tubular folds formed by the combination of shear along stream lines that crosscut the layering with a concomitant tangential shortening along the developing folds were described by Talbot & Jackson (1987) from the bottom of salt diapirs (see especially their fig. 13). The radial flow of salt from a horizontal source layer towards the vertical cylindrical stem of the diapir

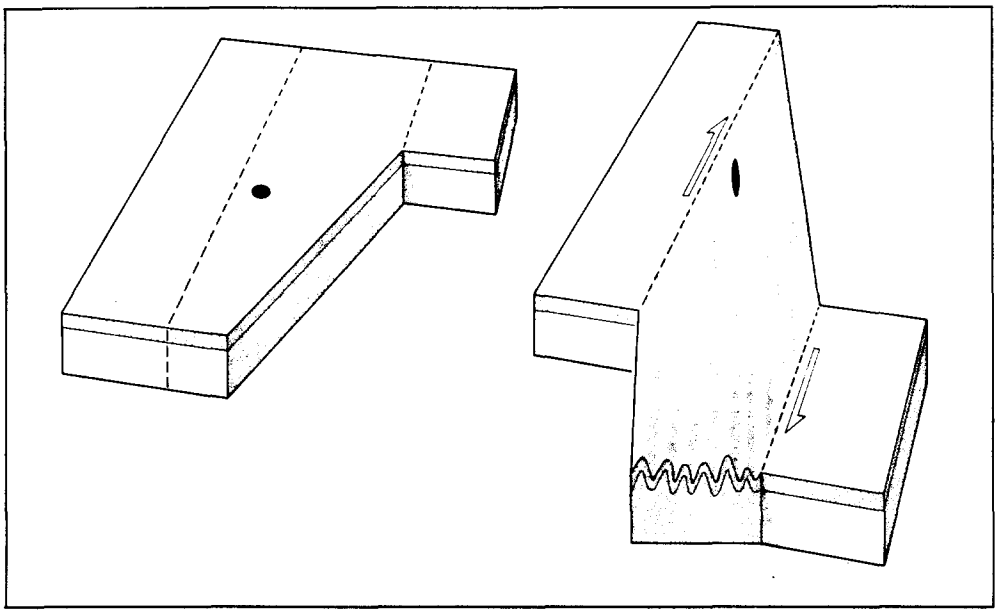

Fig. 9. Development of transverse folds in steep wrench shear zones. Left block before shearing, right block after a shear of $\gamma = 3$. Drawn in perspective.

involves a pronounced tangential contraction. Such large shortening at right angles to the flow direction is hardly likely during nappe emplacement.

Another place where transverse folds may develop is in temporary ductile lateral or oblique ramps, i.e. in strike-slip shear zones at large angles to the orogenic front (see Fig. 9 and Meneilly & Storey 1986). Such shear zones may form the link between two nappe sections that moved with different velocities (Coward 1984) or they may be ductile equivalents of tear faults (cf. Leon & Choukroune 1980, Fischer & Coward 1982, Rattey & Sanderson 1982, Ridley 1982, Coward & Potts 1983, Lagarde & Michard 1986, Brun & Merle 1988).

Folds that are formed in strike-slip shear zones like those shown in Fig. 9 start with their axes in the extension field of the strain ellipsoid. A strike-slip shear of $\gamma = 3$ would cause a maximum shortening of 70% in a direction 73° from the shearing direction. The resulting folds would have axial directions at an angle between 14 and 17° to the shearing direction, and the extension along the fold axes would be about 190–230%. The variation is due to uncertainty as to whether the folds are rotated as passive markers or whether they follow the maximum extension direction. Brun & Merle (1988) produced transverse folds in wrench shear zones; these folds were initiated over longitudinal ridges in the floor.

The amounts of stretching and rotation involved in the formation of transverse folds in ductile wrench shear zones are not nearly as large as would be the case if the transverse folds had originated parallel to the nappe front and were later rotated during a roughly layer-parallel simple shear (Meneilly & Storey 1986).

If the transverse folds develop axial culminations and depressions, as they probably do—at least at the borders of the strike-slip shear zone or if they interfere with crossing folds, they may evolve to form tubular folds when the 'normal' overall layer-parallel simple shear is superimposed on them. Sanderson (1982) gave mathematical solutions to strain calculations for combined wrench- and thrust-type shear.

TUBULAR FOLDS IN THE GRAPESVARE AREA

The Grapesvare area is situated in northern Sweden, just north of the Arctic Circle and about 30 km from the national border between Sweden and Norway. Tectonically it lies within the Caledonian Seve nappe northeast of the Nasafjäll window. The area has been described by Kulling (1982) and Andreasson *et al.* (1985). Dallmeyer & Gee (1986) give an account of the Caledonian framework and evolution.

The dominant lithological units of the Grapesvare area are a semipelitic mica schist and a layered feldspathic quartzite, called the Juron quartzite by Kulling (1982), which in high-strain zones are transformed to flagstones. Folded primary sedimentary structures recognizable in a few localities pass laterally into the general layering of the quartzite (fig. 5 in Andreasson *et al.* 1985). In the mica schist the original sedimentary layering is completely transposed, except perhaps in occasional quartz-banded parts of the unit, where however the origin of the quartz bands is uncertain. The Grapesvare area is known for its boudins of eclogite and metadolerite (see the references given above) which may have introduced heterogeneities into the deformation.

With few exceptions, the occurrence of tubular folds in the area is confined to the banded feldspathic quartzite, probably because the layered structure promoted an early active folding, while the mica schist was passively rotated and homogeneously shortened. The various amounts of penetrative strain that were taken up by the two rock types may also have led to obliteration of early formed tubular folds in the mica schist. In one or

two places tubular folds have been found in quartz-banded varieties of the mica schist.

The meso- and microstructures of the Seve nappe in general show that it has suffered a relatively large penetrative shear strain which was heterogeneous with respect to intensity. Narrow internal high shear 'thrust' zones bound 'thrust slices' that show lower internal strain (Zwart 1974, Williams & Zwart 1977). Williams & Zwart mentioned rotational strains that have resulted in maximum shortening up to 90%. In simple shear this would need a shear strain of 10, a figure that is in keeping with the formation of tubular folds. Actually much larger strains are probable in the pelites and the flagstones. The main schistosity of the rocks was developed by this penetrative deformation during the emplacement of the nappe. Williams & Zwart (1977) divided the folds of the Seve nappe into two groups. Group 1 contains several generations of mesoscale folds, all of which contribute to the regional foliation, although the exact relationship between folds and foliation is not straightforward. Group 1 folds are reclined cylindrical or non-cylindrical folds or even tubular folds. They are thought to have originated before or during the nappe emplacement.

Group 2 folds comprise both meso- and macrofolds that clearly fold the regional foliation as well as the internal high strain zones.

Shape determinations

The broad division of folds into Group 1 and 2 as described in Williams & Zwart (1977) is more appropriate for the structures in the Grapesvare area than the usual classification of folds as belonging to separate well defined fold phases. When two folds seem to belong to the same fold phase, one of them may be older and the other one younger than two other folds that would also be viewed as belonging to one fold phase. The consequence of this would be the establishment of a large number of fold phases. It is concluded that during the nappe emplacement, folds were continuously formed as a result of internal ductile deformation in the nappe. While folds with one axial direction formed in one part of the nappe, folds with another axial direction formed at the same time in another place and vice versa. Even the tubular folds probably developed continuously whenever the appropriate geometrical configurations arose somewhere in the deforming system.

Except for some open late folds, the mesoscale folds in the Grapesvare area, including the tubular folds, belong to the Group 1 folds of Williams & Zwart. In the tubular folds the cleavage is always subparallel to the xy section of the fold (see Fig. 13). In other mesoscale folds the cleavage is axial planar, but in some cases two generations of cleavage were recognized. The older of these was folded by the folds to which the younger cleavage is axial planar. Except in fold hinges both cleavages contribute to the regional foliation. Stretching lineations are subparallel to the fold axes but small deviations are commonly seen. In tubular folds the lineation is mostly subparallel to one hinge line rather than to the central cone axis. Two lineations at a small angle to each other were observed in some places.

Shape parameters from a total of 54 tubular folds or other sheath folds were measured. Eight samples containing 12 tubular folds were sliced and thoroughly examined. The others were measured in the field and on photos. Some occurred in talus blocks. $z:y$ ratios were measured in sections thought to be at right angles to the cone axis, but when the exact position of this was not known the orientation of the lineation was taken as a sufficiently accurate indicator. In some cases $z:y$ ratios were calculated from measurements on slightly oblique sections. In some asymmetric tubular folds it was difficult to establish the exact position of the z and y axes.

The spread of 140 $z:y$ ratios from the 54 folds is from 0.08 to 1.00 with most values lying between 0.2 and 0.6 (Fig. 10b). For different layers in one fold the deviation seldom exceeds 0.15, which indicates that layer thicknesses generally vary around the fold in accordance with the $z:y$ ratio (compare with equation A20 in the Appendix). Exceptions to this are however not uncommon. There is no general trend in the variation of $z:y$ from outer to inner layers in the folds. Because of the limited number of measurements and the possibilities of minor errors only an incomplete picture of the tubular fold shapes in the area has been obtained, which is however thought to illustrate the general trend (Fig. 10).

ω angles were measured on 25 layers in the 12 tubular folds and are all less than 20°, except one where only the apex area was enclosed in the sample (fold 5C, Fig. 10a). As in each fold x values exceed y values, the structures really are tubular folds in accordance with the definition given in this paper.

In the field hinge line angles were measured in six tubular folds, mostly from talus blocks. The values range from 2 to about 20°, except for one of 50° that was probably measured near the apex. The presence of tubular folds pointing in opposite directions was established in some cases. In sample 3 (Fig. 13e) two tubular folds that point in the same direction have parallel axes, while the third, that is opposite, has an axis at 7° to the others. Mesoscale folds other than tubular folds are often subparallel to the hinge lines of nearby tubular folds.

The tubular folds in the Grapesvare area most probably originated by shearing of the types of structure shown in Figs. 5 and 8 or from shearing of more complex interference patterns (compare Figs. 12 and 13 with Figs. 5, 6 and 8). In either case the development of transverse folds with their axes more or less parallel to the shearing direction seems to be a prerequisite for the formation of the tubular folds. The transverse folds may have formed in regions which have accommodated a component of pure shear with a shortening parallel to the length of the Caledonides, or they may have formed in strike-slip shear zones in the manner illustrated in Fig. 9. Strike-slip shear zones at large angles to the Caledonian front have been reported from the Maddåive area only 20 km west of Grapesvare (Nordgren 1987).

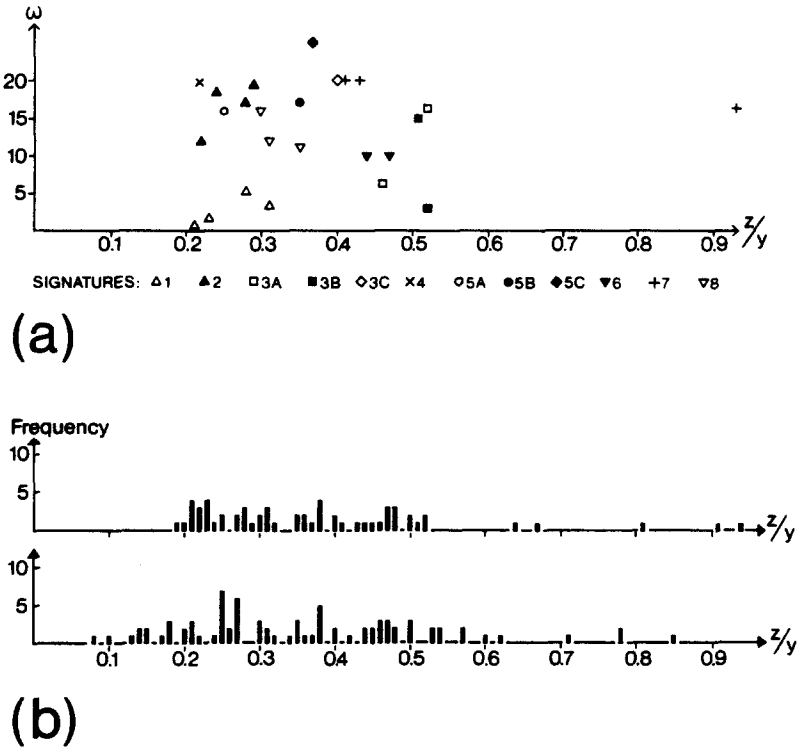

Fig. 10. (a) Plot showing ω and $z:y$ values from 12 tubular folds contained in eight samples. Symbols refer to different tubular folds. 3A, 3B and 3C are different folds from one sample, as also are 5A, 5B and 5C. (b) Histograms showing $z:y$ values measured in samples (upper histogram) and in the field and from photos (lower histogram).

Orientation of mesoscale structures

The orientation of both the tubular folds and other mesoscopic folds in the Grapesvare area remains somewhat puzzling. In other parts of the Seve nappe the tubular folds together with other 'transversal' folds are oriented approximately perpendicular to the orogenic front (Williams & Zwart 1977), as should also be expected from the model presented in this paper. Even in the nearby Maddåive area rare sheath folds and tight recumbent so-called F_1 folds in the Juron quartzite have axes plunging WNW subparallel to the inferred shearing direction during the overthrusting of the nappes (Nordgren 1987). However, in the Grapesvare area the tubular folds, together with recumbent mesoscale folds, mostly plunge in directions between 45 and 90° (see Fig. 11 and Andreasson *et al.* 1985, fig. 3).

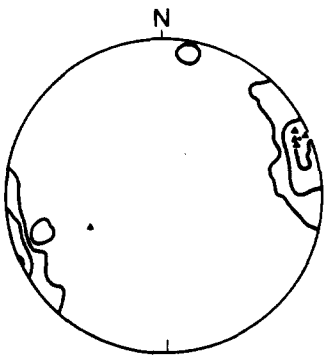

Fig. 11. Contoured stereographic plot showing distribution of axes of 67 mesoscopic folds from a small part of the Grapesvare area. Contours at 2%, 10% and 25%. Triangles mark the orientation of five tubular fold axes. The tubular fold with a steep plunge to the WSW is disturbed by scar folding between eclogite boudins.

This discrepancy could be explained by a speculative model involving late large-scale folding of the area around E–W axes. Kulling (1982) described the Juron quartzite as lying in the core of a major recumbent antiform, the orientation of which is however not clear from his description. The unravelling of the major structures should be given a high priority in future mapping projects in the area.

The macrofolds (km size) of the Grapesvare area are S-verging recumbent folds with E–W axes overprinted by open E–W folds (F_2 and F_3 of Andreasson *et al.* 1985). The abnormal orientation of the tubular folds and related mesoscale folds could be the result of a simple rotation of the layers containing them into the inverted limb of a major recumbent fold with E–W axis. This would imply that the investigated area is inverted and occupies the lower limb of a macroscopic recumbent anticlinorium with the large F_2 folds of Andreasson *et al.* (1985) as the parasitic second-order folds. As the large recumbent folds have not only rotated earlier mesoscale structures, but also folded the regional foliation and the flagstones of the high strain zones, they belong to the Group 2 of Williams & Zwart (1977) and must have formed after the main nappe emplacement. It is suggested that the late recumbent macrofolds were formed in a wide dextral strike-slip shear zone at large angles to the orogenic front in the way illustrated in Fig. 9, the strike-slip shear being combined with a component

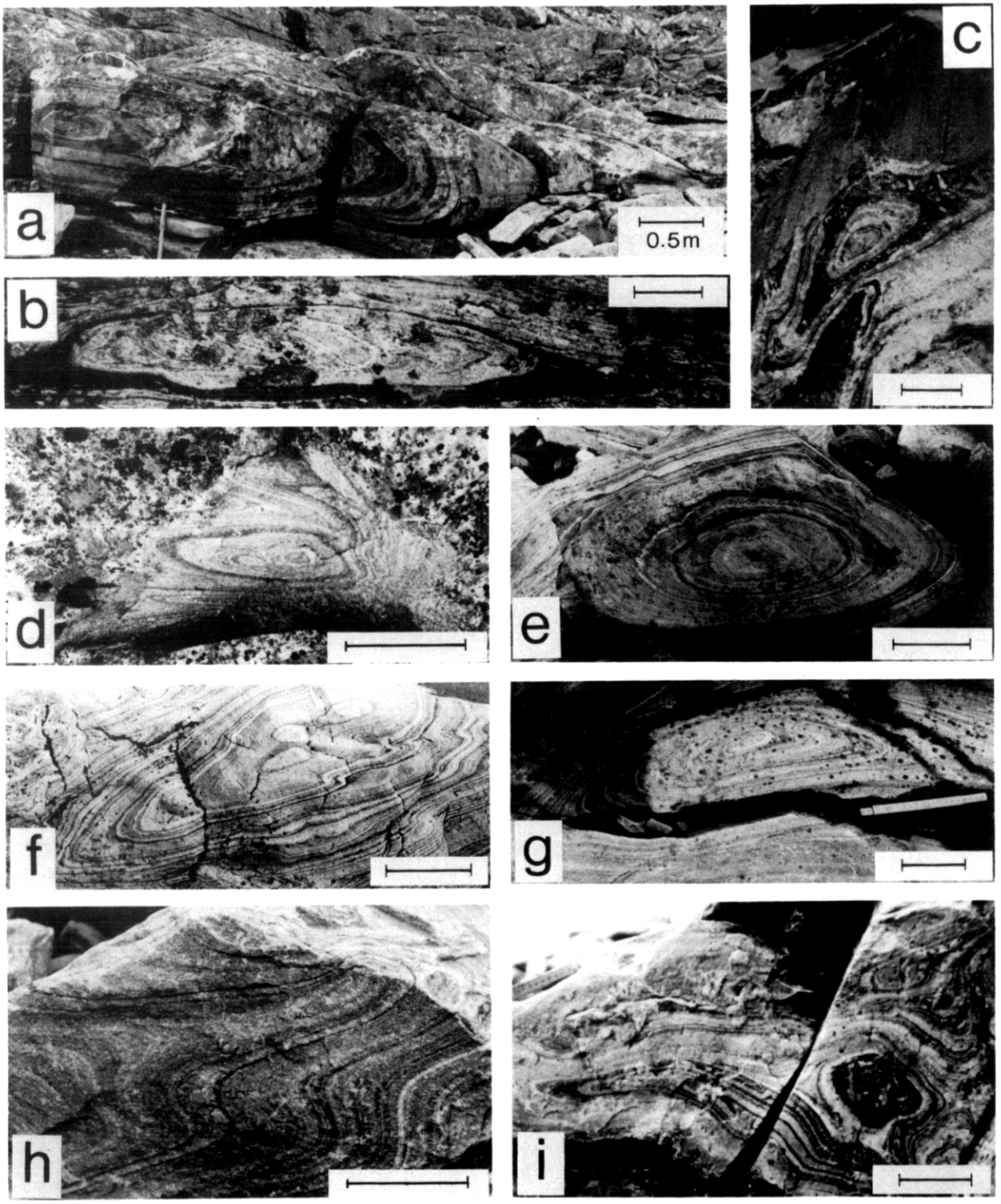

Fig. 12. Examples of tubular folds from the Grapesvare area; compare with Figs. 5, 6 and 8. (d) Shows exposure after sample 5 was removed (cf. Fig. 10a). Scale bars in (b)–(i) are 10 cm.

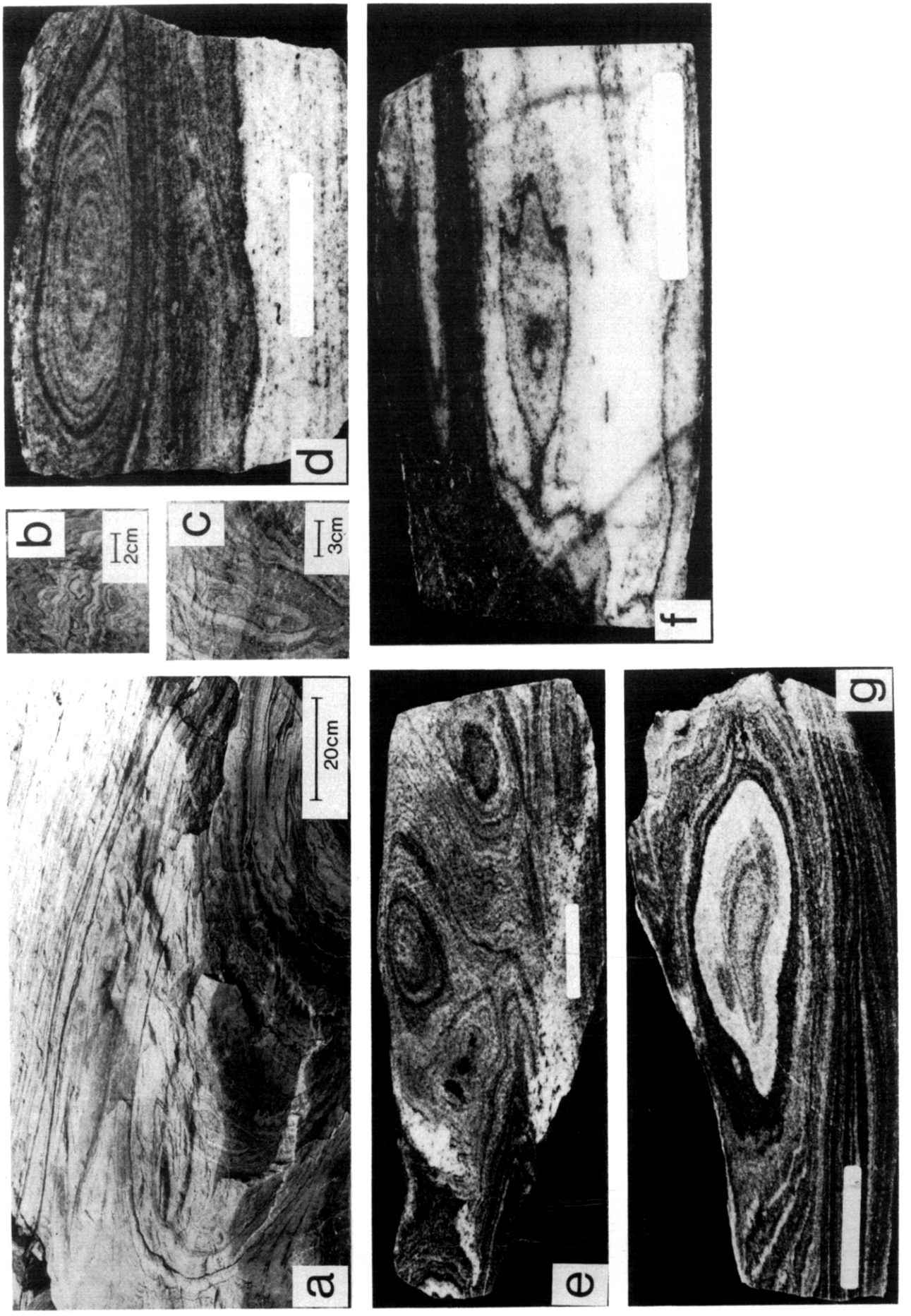

Fig. 13. Examples of tubular folds from the Grapesvare area. (b) and (c) are enlarged details from (a). (d)–(g) are of cut and polished samples; the white bars are 3 cm. (d) Sample 1, (e) sample 3, (f) sample 8, (g) sample 2. Compare with Fig. 10 (a).

of concomitant shear along horizontal shear planes that has overturned the folds. If the main orientation of the layering was not horizontal prior to the dextral shearing, but had a small dip towards the hinterland, this would have contributed to the overturning of the folds. Stretching lineations were developed subparallel to the fold axes, and older lineations and mesoscale folds were not only bodily rotated around the new fold axes, but also stretched as they were passively rotated towards the younger axes (cf. Saure 1985). A dextral shear of $\gamma = 2$ in an ESE direction would result in folding around roughly E–W axes with an extension of about 130–140% along the axes. It is therefore unlikely that the E–W folds originated with axes parallel to the nappe front.

CONCLUSIONS

(1) A tubular fold is defined as a highly non-cylindrical cone-shaped fold with hinge line angle $\omega < 20°$ and for which a cross-section can be drawn so that ω at the cross-section is less than 20° and the $x:y$ ratio is >1 (see Fig. 1a). The corresponding values for sheath folds are $\omega < 90°$ and $x:y > 1/4$.

(2) In shearing environments tubular folds may develop by the superposition of an overall layer-parallel simple shear on transverse non-cylindrical structures (i.e. structures with elongation at a small angle to the shearing direction). These may either be transverse folds with axial culminations and depressions or interference structures. The general trend of the non-cylindrical parts of the structural progenitors must be close to parallel to the later shearing direction.

(3) Tubular folds cannot develop by the superposition of simple shear on previous subcircular layer irregularities or subhorizontal longitudinal folds (i.e. folds with axes subperpendicular to the shearing direction). Transverse folds are a prerequisite for the formation of tubular folds in simple shear environments.

(4) Transverse folds must either have formed at a small angle to the later shearing direction or have been oriented at a high angle to the shear plane before their rotation towards the shearing direction.

(5) Transverse folds may be the result of local shortening along the orogen or they may have originated in ductile strike-slip zones at large angles to the orogenic front.

(6) Tubular folds from the Grapesvare area fulfil the definition given above and occur in a structural setting that fits with models described.

(7) The orientations of mesoscale folds, including tubular folds, in the Grapesvare area indicate that during the last stage of the emplacement of the Seve nappe, internal ductile strike-slip shear along a wide transverse zone overshadowed the 'normal' thrust-related internal shear in the area.

Acknowledgements—Thanks are especially due to P. G. Andreasson who introduced me to the Grapesvare area and to C. J. Talbot, Carol Simpson, Maria Nordgren, T. C. R. Pulvertaft and an unknown reviewer for critically reading the manuscript. T. C. R. Pulvertaft and C. J. Talbot improved the English. René Madsen drafted the figures and made the perspective constructions. Photographs by O. Bang Berthelsen, Pernille Anderson typed the manuscript, Maria Nordgren and Olav Hansen assisted me in the field. Thanks are due to them all. The field work was funded by the Danish Natural Science Research Council.

REFERENCES

Agar, S. M. 1988. Shearing of partially consolidated sediments in a lower trench slope setting, Shimanto Belt, SW Japan. *J. Struct. Geol.* **10**, 21–32.

Andreasson, P.-G., Gee, D. G. & Sukotjo, S. 1985. Seve eclogites in the Norrbotten Caledonides, Sweden. In: *The Caledonide Orogen—Scandinavia and Related Areas* (edited by Gee, D. G. & Sturt, B. A.). J. Wiley and Sons, Chichester, 887–901.

Balk, R. 1953. Salt structure of Jefferson Island salt dome, Iberian and Vermilion Parishes, Louisiana. *Bull. Am. Ass. Petrol. Geol.* **37**, 2455–2474.

Berthé, D. & Brun, J. P. 1980. Evolution of folds during progressive shear in the South Armorican Shear Zone, France. *J. Struct. Geol.* **2**, 127–133.

Bhattacharji, S. 1958. Theoretical and experimental investigations on cross-folding. *J. Geol.* **66**, 625–667.

Borradaile, G. J. 1972. Variably oriented co-planar primary folds. *Geol. Mag.* **109**, 89–98.

Brun, J. P. & Merle, O. 1988. Experiments on folding in spreading-gliding nappes. *Tectonophysics* **145**, 129–139.

Bryant, B. & Reed, J. C. 1969. Significance of lineation and minor folds near major thrust faults in the southern Appalachians and the British and Norwegian Caledonides. *Geol. Mag.* **106**, 412–429.

Butler, W. H. 1982. Hangingwall strain: a function of duplex shape and footwall topography. *Tectonophysics* **88**, 235–246.

Carey, S. W. 1962. Folding. *J. Alberta Soc. Petrol. Geol.* **10**, 95–144.

Carmignani, L., Giglia, G. & Kligfield, R. 1978. Structural evolution of the Apuane Alps: an example of continental margin deformation in the northern Apennines, Italy. *J. Geol.* **86**, 487–504.

Carreras, J., Estrada, A. & White, S. 1977. The effect of folding on the *c*-axis fabrics of a quartz mylonite. *Tectonophysics* **39**, 3–24.

Cobbold, P. R. & Quinquis, H. 1980. Development of sheath folds in shear regimes. *J. Struct. Geol.* **2**, 119–126.

Coward, M. P. 1984. The strain and textural history of thin-skinned tectonic zones: examples from the Assynt region of the Moine thrust zone, NW Scotland. *J. Struct. Geol.* **6**, 89–99.

Coward, M. P. & Potts, G. J. 1983. Complex strain patterns developed at the frontal and lateral tips to shear zones and thrust zones. *J. Struct. Geol.* **5**, 383–399.

Dallmeyer, R. D. & Gee, D. G. 1986. Polyphase Caledonian orogenesis within the Baltoscandian Miogeosyncline: evidence from $^{40}Ar/^{39}Ar$ mineral dates from retrogressed eclogites. *Bull. geol. Soc. Am.* **97**, 26–34.

Dalziel, I. W. D. & Bailey, S. W. 1968. Deformed garnets in a mylonitic rock from the Grenville Front and their tectonic significance. *Am. J. Sci.* **266**, 542–562.

Escher, A. & Watterson, J. 1974. Stretching fabric, folds and crustal shortening. *Tectonophysics* **22**, 223–231.

Ewans, D. J. & White, S. H. 1984. Microstructural and fabric studies from the rocks of the Moine Nappes, Eribol, NW Scotland. *J. Struct. Geol.* **6**, 369–389.

Faure, M. 1985. Microtectonic evidence for eastward ductile shear in the Jurassic orogen of SW Japan. *J. Struct. Geol.* **7**, 175–186.

Fischer, M. W. & Coward, M. P. 1982. Strains and folds within thrust sheets: an analysis of the Heilam sheet, northwest Scotland. *Tectonophysics* **8**, 291–312.

Gaudemer, Y. & Tapponnier, P. 1987. Ductile and brittle deformations in the northern Snake Range, Nevada. *J. Struct. Geol.* **9**, 159–180.

Gee, D. G. & Sturt, B. A. (eds) 1985. *The Caledonide Orogen—Scandinavia and Related Areas*. J. Wiley and Sons, Chichester.

Ghosh, S. K. & Sengupta, S. 1984. Successive development of plane noncylindrical folds in progressive deformation. *J. Struct. Geol.* **6**, 703–709.

Ghosh, S. K. & Sengupta, S. 1987. Progressive development of structures in a ductile shear zone. *J. Struct. Geol.* **9**, 277–287.

Hanmer, S. 1986. Asymmetrical pull-aparts and foliation fish as kinematic indicators. *J. Struct. Geol.* **8**, 111–122.

Hansen, E. 1971. *Strain Facies*. Springer-Verlag, New York.
Henderson, J. R. 1981. Structural analysis of sheath folds with horizontal *X*-axes, northeast Canada. *J. Struct. Geol.* **3**, 203–210.
Henderson, J. R. 1983. Structure and metamorphism of the Aphebian Penrhyn group and its Archaean basement complex in the Lyon Inlet area, Melville peninsula, district of Franklin. *Bull. Geol. Surv. Can.* **324**, 50.
Hibbard, J. & Karig, D. E. 1987. Sheath-like folds and progressive fold deformation in Tertiary sedimentary rocks of the Shimanto accretionary complex, Japan. *J. Struct. Geol.* **9**, 845–857.
Hudleston, P. J. 1977. Similar folds, recumbent folds and gravity tectonics in ice and rocks. *J. Geol.* **85**, 113–122.
Kulling, O. 1982. Översikt över södra Norrbottensfjällens Kaledonberggrund. *Sver. geol. Unders. Ba* **26**, 1–29.
Lagarde, J. L. & Michard, A. 1986. Stretching normal to the regional thrust displacement in a thrust-wrench shear zone, Rehamna Massif, Morocco. *J. Struct. Geol.* **8**, 483–492.
Leon, M. J. P. & Choukroune, P. 1980. Shear zones in the Iberian Arc. *J. Struct. Geol.* **2**, 63–68.
Lisle, J. 1984. Strain discontinuities within the Seve-Köli Nappe Complex, Scandinavian Caledonides. *J. Struct. Geol.* **6**, 101–110.
Lister, G. S. & Price, G. P. 1978. Fabric development in a quartz-feldspar mylonite. *Tectonophysics* **49**, 37–78.
Malavieille, J. 1987. Kinematics of compressional and extensional ductile shearing deformation in a metamorphic core complex of the northeastern Basin and Range. *J. Struct. Geol.* **9**, 541–554.
Marcoux, J., Brun, J.-P., Burg, J.-P. & Ricou, L. E. 1987. Shear structures in anhydrite at the base of thrust sheets (Antalya, Southern Turkey). *J. Struct. Geol.* **9**, 555–561.
Mattauer, M., Faure, M. & Malavieille, J. 1981. Transverse lineation and large-scale structures related to Alpine obduction in Corsica. *J. Struct. Geol.* **3**, 401–409.
Meneilly, A. W. & Storey, B. C. 1986. Ductile thrusting within subduction complex rocks on Signy Island, South Orkney Islands. *J. Struct. Geol.* **8**, 457–472.
Mertie, J. B. 1957. Classification, delineation, and measurement of nonparallel folds. *Prof. Pap. U.S. geol. Surv.* **314**, 91–121.
Minnigh, L. D. 1979. Structural analysis of sheath-folds in a meta-chert from the Western Italian Alps. *J. Struct. Geol.* **1**, 275–282.
Nicholson, R. 1963. Eyed folds and interference patterns in the Sokumfjell marble group, northern Norway. *Geol. Mag.* **100**, 59–70.
Nordgren, M. 1987. Deformation structures in the trailing part of a Seve lens, Maddåive, Scandinavian Caledonides. Unpublished thesis, Geologisk Centralinstitut, University of Copenhagen.
Olesen, N. Ø. & Sørensen, K. 1972. Caledonian fold- and fabric-elements: A model. *Proc. 24. Int. Geol. Congr.* Section 3, 533–544.
Platt, J. P. & Lister, G. S. 1985. Structural evolution of a nappe complex, southern Vanoise massif, French Penninic Alps. *J. Struct. Geol.* **7**, 145–160.
Price, R. A. 1972. The distinction between displacement and distortion in flow, and the origin of diachronism in tectonic overprinting in orogenic belts. *Proc. 24. Int. Geol. Congr.* Section 3, 545–551.
Quinquis, H., Audren, C., Brun, J. P. & Cobbold, P. R. 1978. Intense progressive shear in Ile de Groix blueschists and compatibility with subduction or obduction. *Nature* **273**, 43–45.
Quirke, T. T. & Lacy, W. C. 1941. Deep-zone dome and basin structures. *J. Geol.* **49**, 589–609.
Ragan, D. M. 1985. *Structural Geology. An Introduction to Geometrical Techniques* (3rd edn). J. Wiley & Sons, Chichester.
Ramberg, H. & Ghosh, K. 1977. Rotation and strain of linear and planar structures in three-dimensional progressive deformations. *Tectonophysics* **40**, 309–337.
Ramsay, D. M. & Sturt, B. A. 1973. An analysis of noncylindrical and incongruous fold pattern from the Eo-Cambrian rocks of Söröy, Northern Norway. I. Noncylindrical, incongruous and aberrant folding. *Tectonophysics* **18**, 81–107.
Ramsay, J. G. 1958. Superimposed folding at Loch Monar, Inverness-shire and Ross-shire. *Q. Jl geol. Soc. Lond.* **113**, 271–307.
Ramsay, J. G. 1962. Interference patterns produced by the superposition of folds of similar type. *J. Geol.* **70**, 466–481.
Ramsay, J. G. 1980. Shear zone geometry: a review. *J. Struct. Geol.* **2**, 83–89.
Ramsay, J. G. & Huber, M. J. 1987. *The Techniques of Modern Structural Geology. Volume 2: Folds and Fractures*. Academic Press, London.
Rattey, P. R. & Sanderson, D. J. 1982. Patterns of folding within nappes and thrust sheets: examples from the Variscan of southwest England. *Tectonophysics* **88**, 247–267.
Ridley, J. 1982. Arcuate lineation trends in a deep level, ductile thrust belt, Syros, Greece. *Tectonophysics* **88**, 347–360.
Sanderson, D. J. 1982. Models of strain variation in nappes and thrust sheets. *Tectonophysics* **88**, 201–233.
Skjernaa, L. 1980. Rotation and deformation of randomly oriented planar and linear structures in progressive simple shear. *J. Struct. Geol.* **2**, 101–109.
Talbot, C. J. 1979. Fold trains in a glacier of salt in southern Iran. *J. Struct. Geol.* **1**, 5–18.
Talbot, C. J. & Jackson, M. P. A. 1987. Internal kinematics of salt diapirs. *Bull. Am. Ass. Petrol. Geol.* **71**, 1068–1093.
Tobisch, O. T. 1966. Large-scale basin-and-dome pattern resulting from the interference of major folds. *Bull. geol. Soc. Am.* **77**, 393–408.
Williams, G. D. 1978. Rotation of contemporary folds into the X direction during overthrust processes in Laksefjord, Finnmark. *Tectonophysics* **48**, 29–40.
Williams, G. D. & Chapman, T. J. 1979. The geometrical classification of noncylindrical folds. *J. Struct. Geol.* **1**, 181–185.
Williams, P. F. & Zwart, H. J. 1977. A model for the development of the Seve-Köli Caledonian nappe complex. In: *Energetics of Geological Processes* (edited by Saxena, S. K. & Bhattacharji, S.). Springer-Verlag, New York, 169–187.
Zwart, H. J. 1974. Structure and metamorphism in the Seve-Köli nappe complex (Scandinavian Caledonides) and its implications concerning the formation of metamorphic nappes. *Centrenaire Soc. Géol. Belgique Géol. Dom. Crist., Liege*, 129–144.

APPENDIX

Layer-parallel simple shear superposed on domal structures and periclinal folds

Figures A1(a) and A2(a) show sections through a domal structure cut parallel to the *ac* plane and *bc* plane, respectively, of the simple shear that is to be superposed on it; *a*, *b* and *c* are the kinematic axes of the simple shear. Figures A1(b) and A2(b) show the same sections through the structure after it has been subjected to a horizontal simple shear with $\gamma = 2.5$ (notice that dextral shears have positive values).

From these cross-sections it is possible by simple trigonometric calculations, combined with well known equations for simple shear, to relate the shape of the sheared dome to its original shape and to γ. The designations of the different angles and line segments are given in the figures. The interlimb angle β (in Fig. A2b) is in this case the angle ω.

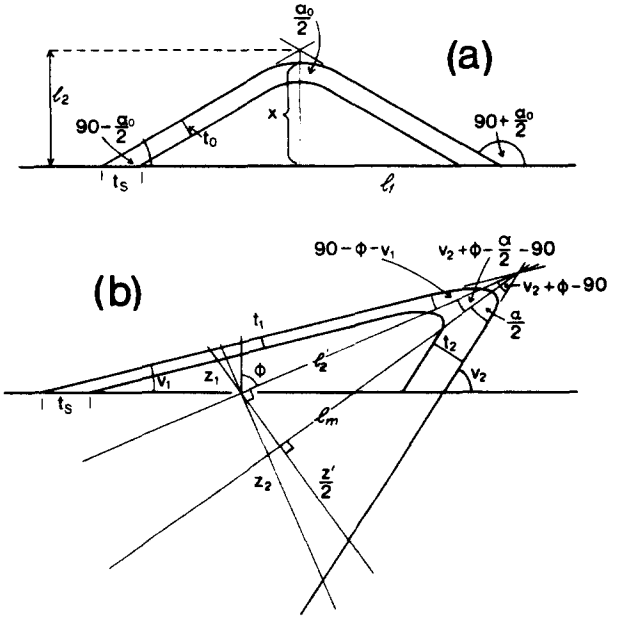

Fig. A1. Definition of geometrical elements in sections cut parallel to the *ac*-kinematic plane of a horizontal dextral simple shear. (a) Before shear. (b) After shear.

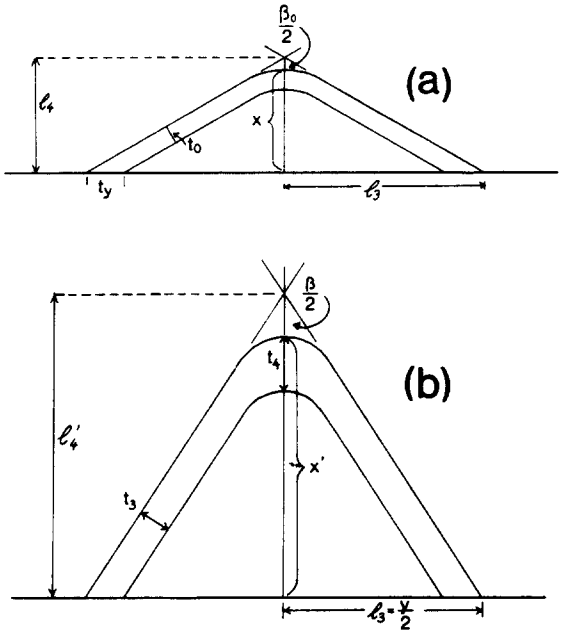

Fig. A2. Definition of geometrical elements. (a) Section through the dome before shear, the section is perpendicular to the section shown in Fig. A1(a), the two sections share the x axis. (b) Same section as in (a) but after shear; the section is perpendicular to the section shown in Fig. A1(b) and contains the l_2' direction.

The equations derived below are valid both for domes and basins (in which case $\alpha_0 = \beta_0$ and $l_1 = l_3$) and for periclinal folds with their main axes either parallel to or at right angles to the a-kinematic axis.

To find the apical angles α and β:

Combining Figs. A1(a) & (b) with the general equation for rotation of lines in the ac plane (Ramsay 1980, p. 90) one can write:

$$\cot \nu_1 = \cot\left(90 - \frac{\alpha_0}{2}\right) + \gamma = \tan\frac{\alpha_0}{2} + \gamma \tag{A1}$$

$$\cot \nu_2 = \cot\left(90 + \frac{\alpha_0}{2}\right) + \gamma = -\tan\frac{\alpha_0}{2} + \gamma \tag{A2}$$

$$\alpha = \nu_2 - \nu_1. \tag{A3}$$

From Figs. A2(a) and (b):

$$l_4 = l_3\left(\tan\frac{\beta_0}{2}\right)^{-1} \tag{A4}$$

$$l_4' = l_3\left(\tan\frac{\beta}{2}\right)^{-1} = l_4(\cos\varphi)^{-1} \quad \text{(see Fig. A1b)} \tag{A5}$$

$$\tan\frac{\beta}{2} = \tan\frac{\beta_0}{2}\cos\varphi \tag{A6}$$

To find the ratio $z:y$ and layer thicknesses:

The $z:y$ ratio in the monoclinic symmetric non-cylindrical fold can be measured either in a section at right angles to the central axis of the original dome (after shearing the l_2' axis of Fig. A1b) or at right angles to the bisector of the apical angle (the l_m axis of Fig. A1b), in which case z is replaced by z'.

For small values of α (e.g. $\alpha < 20°$ as in tubular folds) the difference between the two measurements is insignificant (a few % if $\alpha = 20°$ and γ is large). For larger values of α, $z':y$ will give the more appropriate value and in some instances be the only one possible because z does not cut the lower limb of the fold.

From Figs. A1(a) & (b):

$$\frac{z_1}{l_2'} = \tan(90 - \varphi - \nu_1) = \cot(\varphi + \nu_1) \tag{A7}$$

$$\frac{z_2}{l_2'} = \tan(\nu_2 + \varphi - 90) = -\cot(\varphi + \nu_2) \tag{A8}$$

$$z = z_1 + z_2 = l_2'(\cot(\varphi + \nu_1) - \cot(\varphi + \nu_2)),$$

as

$$l_2' = l_2(\cos\varphi)^{-1} = l_1\left(\tan\frac{\alpha_0}{2}\cos\varphi\right)^{-1} \tag{A9}$$

and

$$y = 2l_3 \tag{A10}$$

it follows that:

$$\frac{z}{y} = l_1(\cot(\varphi + \nu_1) - \cot(\varphi + \nu_2))\left(2l_3\cos\varphi\tan\frac{\alpha_0}{2}\right)^{-1}. \tag{A11}$$

Equation (A11) is not valid for $\alpha_0 = 0$ (isoclinal folds), but the value of $z:y$ in this case will differ insignificantly from the value obtained by putting for example $\alpha_0 = 0.1$ into equation (A11).

From Fig. A1(b):

$$\cos\left(\nu_2 + \varphi - \frac{\alpha}{2} - 90\right) = \frac{l_m}{l_2'}$$

$$l_m = l_2'\sin\left(\nu_2 + \varphi - \frac{\alpha}{2}\right)$$

$$\frac{z'}{2} = l_m\tan\frac{\alpha}{2}$$

$$z' = 2l_2'\tan\frac{\alpha}{2}\sin\left(\nu_2 + \varphi - \frac{\alpha}{2}\right).$$

Combining this with equations (A9) and (A10) gives:

$$\frac{z'}{y} = \frac{l_1\sin\left(\nu_2 + \varphi - \frac{\alpha}{2}\right)\tan\frac{\alpha}{2}}{l_3\tan\frac{\alpha_0}{2}\cos\varphi}. \tag{A12}$$

From Figs. A1(a) & (b):

$$t_s = t_0\left(\cos\frac{\alpha_0}{2}\right)^{-1} = t_1(\sin\nu_1)^{-1}$$

$$\frac{t_1}{t_0} = \sin\nu_1\left(\cos\frac{\alpha_0}{2}\right)^{-1} \tag{A13}$$

$$\frac{t_2}{t_0} = \sin\nu_2\left(\cos\frac{\alpha_0}{2}\right)^{-1}. \tag{A14}$$

Note that t_1 and t_2 are the orthogonal thicknesses of the layers. For values of $\alpha < 20°$ the difference between these and the thicknesses parallel to z is however <1.6%.

From Figs. A2(a) & (b):

$$t_y = t_0\left(\cos\frac{\beta_0}{2}\right)^{-1} = t_3\left(\cos\frac{\beta}{2}\right)^{-1} \tag{A15}$$

$$\frac{t_3}{t_0} = \cos\frac{\beta}{2}\left(\cos\frac{\beta_0}{2}\right)^{-1} \tag{A16}$$

$$\frac{t_4}{t_0} = \frac{l_4'}{l_4} = (\cos\varphi)^{-1} \tag{A17}$$

$$\frac{t_1}{t_y} = \sin\nu_1\cos\frac{\beta_0}{2}\left(\cos\frac{\alpha_0}{2}\right)^{-1} \tag{A18}$$

$$\frac{t_2}{t_y} = \sin\nu_2\cos\frac{\beta_0}{2}\left(\cos\frac{\alpha_0}{2}\right)^{-1}. \tag{A19}$$

For small values of α, t_1/t_y and t_2/t_y will both be very close to z/y while for greater values of α, $t_1/t_y < z/y$ and $t_2/t_y > z/y$

$$\frac{t_1 + t_2}{2t_y} \sim \frac{z}{y}. \tag{A20}$$